MNRAS **000**, 1–15 (2020) Preprint 13 December 2021 Compiled using MNRAS LATEX style file v3.0

Pulsating B stars in the Scorpio–Centaurus Association with *TESS*

Awshesh N. Sharma[1,2]★, Timothy R. Bedding[2,3]†, Hideyuki Saio[4] and Timothy R. White[2,3]

[1]*Department of Earth Sciences, Indian Institute of Technology Roorkee, Roorkee, Uttarakhand 247667 India*
[2]*Sydney Institute for Astronomy, School of Physics, University of Sydney 2006, Australia*
[3]*Stellar Astrophysics Centre, Department of Physics and Astronomy, Aarhus University, 8000 Aarhus C, Denmark*
[4]*Astronomical Institute, Graduate School of Science, Tohoku University, Sendai 980-8578, Japan*

ABSTRACT

We study 119 B stars located in the Scorpio-Centaurus Association using data from NASA's TESS Mission. We see pulsations in 79 stars across the full range of effective temperatures. In particular, we confirm previous reports of low-frequency pulsations in stars whose temperatures fall between the instability strips of SPB stars (slowly pulsating B stars) and δ Sct stars. By taking the stellar densities into account, we conclude that these cannot be p modes and confirm previous suggestions that these are probably rapidly-rotating SPB stars. We also confirm that they follow two period–luminosity relations that are consistent with prograde sectoral g modes that are dipole ($l = m = 1$) and quadrupole ($l = m = 2$), respectively. One of the stars (ξ^2 Cen) is a hybrid pulsator that shows regular spacings in both g and p modes. We also find several interesting binaries, including a very short-period heartbeat star (HD 132094), a previously unknown eclipsing binary (π Lup), and an eclipsing binary with high-amplitude tidally driven pulsations (HR 5846). The results clearly demonstrate the power of *TESS* for studying variability in bright stars.

Key words: stars: oscillations,

1 INTRODUCTION

The *Transiting Exoplanet Survey Satellite* (*TESS*; Ricker et al. 2015) is providing high-precision photometry for bright stars across a large fraction of the sky, which allows a systematic study of pulsations in nearby stellar associations. We have used *TESS* light curves to examine the variability of more than a hundred B-type stars in the Scorpio–Centaurus Association (Sco–Cen; Sco OB2). This is the nearest OB association, with member stars having ages in the range 5–16 Myr (Blaauw 1946; Jones & Shobbrook 1974; Balona & Feast 1975; de Geus et al. 1989; De Zeeuw et al. 1999; Preibisch & Mamajek 2008; Pecaut & Mamajek 2016; Murphy et al. 2021).

Pulsating B stars are generally divided into two classes. At hotter effective temperatures (spectral types B0–B3) we have the β Cephei stars, which pulsate in low-order pressure modes (p modes; Stankov & Handler 2005; Thoul 2009). At cooler temperatures (typically B3–B8) we find the Slowly Pulsating B-type stars (SPB stars), which pulsate in high-order gravity modes (g modes; Waelkens 1991; De Cat et al. 2011). Both the p and g modes are known to be excited by a heat-engine mechanism acting on the opacities of iron-group elements (Dziembowski & Pamiatnykh 1993; Gautschy & Saio 1993; Dziembowski et al. 1993).

Research into pulsating B stars has been greatly helped by photometry from space missions such as MOST, WIRE, CoRoT, BRITE, *Kepler*/K2, and *TESS* (for reviews, see De Cat et al. 2011; Bowman 2020). Current areas of research include understanding the driving mechanism in the low-metallicity stars of the Magellanic Clouds (Salmon et al. 2012), testing whether opacities need to be modified (Lenz 2011; Moździerski et al. 2019; Daszyńska-Daszkiewicz et al. 2017, 2020), and measuring the amount of internal rotation and mixing (Degroote et al. 2010; Pápics et al. 2017; Pedersen et al. 2021).

Another topic of interest relates to the repeated reports of pulsations in stars that are cooler than expected for SPB stars, with effective temperatures falling between those of SPB stars and δ Sct stars (Handler et al. 2007, 2008; Majewska-Świerzbinowicz et al. 2008; Degroote et al. 2009; Saesen et al. 2010, 2013; Mowlavi et al. 2013, 2016; Moździerski et al. 2014; Lata et al. 2014; Balona et al. 2015, 2016; Daszyńska-Daszkiewicz et al. 2017; Balona & Ozuyar 2020; van Heerden et al. 2020). These have sometimes been called 'Maia variables' but we avoid this term because they have not been established as a separate class of variables (e.g., Aerts & Kolenberg 2005), and also because *Kepler* K2 photometry has shown that Maia itself (20 Tau = HD 23408 in the Pleiades) is not actually a member of the group (White et al. 2017).

The large sky coverage of the *TESS* mission makes it ideally suited to studying B stars (e.g., Balona et al. 2019; Pedersen et al. 2019; Burssens et al. 2020). In this paper, we study variability in

★ E-mail: asharma@es.iitr.ac.in
† E-mail: tim.bedding@sydney.edu.au

119 B-type stars in Sco–Cen using data from *TESS*. We focus on pulsations, but also report on eclipsing binaries and other types of variability.

2 TESS DATA

Our sample of B-type stars in the Sco–Cen Association comes from Rizzuto et al. (2011), with a few additional stars that were considered members by Pecaut & Mamajek (2016). *TESS* covers the sky in partially overlapping sectors, with each sector being observed for about 27 d (two orbits). Note that *TESS* has not yet covered a band within 6° of the ecliptic plane that includes 56 B stars that lie in the Upper Scorpio region of Sco–Cen[1]. This leaves 111 B stars with *TESS* data from Cycle 1, as listed in Table 1. Most were observed in one of Sectors 10, 11 or 12 (which covered from 26 March to 19 June 2019), with 10 stars having observations in both Sectors 10 and 11. We also included 8 B stars that were missed in Cycle 1 (presumably because they landed in gaps between CCDs) but have data in Cycle 3 (Sectors 37, 38 or 39).

The light curves and Fourier amplitude spectra for all stars are shown in the on-line supplementary material. For most stars in our sample, 2-minute *TESS* light curves were available. We used the `lightkurve` package (Lightkurve Collaboration 2018) to download the PDCSAP[2] light curves, which were calculated by the SPOC (Science Processing Operations Center). For 23 stars for which no 2-minute observations were available, we used light curves from the 30-minute full-frame images (FFIs) produced by the MIT Quick Look Pipeline (QLP; Huang et al. 2020).

For β Cen and α Cru, which are two of the brightest stars in the sample and are heavily saturated, we constructed 2-minute light curves ourselves from the pixel-level data. Due to the large size of the target pixel file of β Cen, it was not processed by the TESS photometric pipeline. As a result, not only was there no available SPOC PDCSAP light curve, but the background had not been estimated and subtracted from the flux values in the target pixel file. We estimated the background using the `tessbkgd`[3] python package, and calculated a simple aperture photometry light curve using `lightkurve`. For α Cru, a SPOC PDCSAP light curve was available but the selected pixels did not fully capture the bleed trails that result from saturation, and so aperture losses meant this light curve was of low quality. We instead generated a 'halo' photometry light curve from the unsaturated pixels in the wings of the PSF using the `halophot`[4] package (White et al. 2017; Pope et al. 2019). The light curves for α Cru and β Cen are discussed in Secs. 6.1 and 6.2.

3 STELLAR PROPERTIES

The spectral types, effective temperatures and luminosities for our sample are listed in Table 1. Most spectral types were taken from the five-volume University of Michigan Catalogue (Houk & Cowley 1975; Houk 1978, 1982; Houk & Smith-Moore 1988; Houk & Swift 1999). The exceptions were η Cen, λ Cru and μ Lup, which are known to be emission-line (Be) stars but are not classified as such in the Michigan Catalogue. For these stars we adopted the spectral types measured by Levenhagen & Leister (2006).

We estimated effective temperatures from spectral types using an updated version of Table 5 of Pecaut & Mamajek (2013)[5]. We estimated stellar luminosities from V magnitudes and parallaxes, using bolometric corrections by Pecaut & Mamajek (2013). Note that Gaia parallaxes are not available for some of the brightest stars, so we used Hipparcos parallaxes for the whole sample for consistency. Table 1 also shows the projected rotational velocity ($v \sin i$), which we took as the median of values in the SIMBAD database. For some stars without $v \sin i$ values in SIMBAD, we took measurements directly from the literature (Brown & Verschueren 1997; Wolff et al. 2007; Zorec & Royer 2012; Aerts et al. 2014).

The luminosities and effective temperatures of our sample are plotted in a Hertzsprung–Russell diagram in Fig. 1. We note that binarity is common among B stars (see, for example, Rizzuto et al. 2013), and so it is likely that properties for some stars are affected by binary companions. Discussion of some individual stars is given in Sec. 6.

The evolutionary tracks in Fig. 1 were calculated using Modules for Experiments in Stellar Astrophysics (MESA version 7184; Paxton et al. 2011, 2013, 2015) without rotation, for the chemical composition $(X, Z) = (0.72, 0.014)$ and with OPAL opacity tables. For the convective-core boundary we adopted the Schwarzschild criterion and diffusive overshooting with the parameter $d_{\rm ov} = 0.01$. We estimated the pulsational instability strips for $l = 0$ p modes and $l = 1$ and 2 g modes (red and blue regions in Fig. 1) by carrying out linear non-adiabatic analysis for selected models using the methods of Saio & Cox (1980) for the nonradial pulsations and of Saio et al. (1983) for the radial pulsations.

4 ANALYSIS OF LIGHT CURVES

The light curves and Fourier amplitude spectra for all stars are shown in the Supplementary on-line material. Five of the stars are eclipsing binaries and these are discussed individually in Sec. 6.8. Other light curves show variations typical of rotation or close binary companions, such as 13 Sco, V863 Cen, V1019 Cen, 52 Hya, KT Lup, HD 132094 (a heartbeat star with a very short period; see Sec. 6.4), HD 136482, and HD 143022.

Many stars show clear pulsations and we include four examples in Figs. 2–5. Figure 2 shows the previously-known β Cep star α Lup (HD 129056; B1.5 Vn; Nardetto et al. 2013). Figure 3 shows HR 4879 (HD 111774; B7/8 V), which we find to be an SPB star with two closely-spaced modes. Figure 4 shows ϕ Cen (HD 121743; B2 V), which is seen to be a hybrid pulsator (β Cep and SPB). Finally, Fig. 5 shows HD 115583 (B9 V), which shows clear pulsations with two closely-spaced modes but is cooler that the standard SPB instability strip. We note that fine structure in the oscillation spectra of SPB stars that has been seen with long runs with CoRoT and *Kepler* (e.g. Degroote et al. 2010; Pápics et al. 2017) is not fully resolvable with only two sectors (54 d) of TESS data.

In the H–R diagram (Fig. 1), we have indicated the 79 stars that show pulsations. The theoretical instability strips for β Cep and SPB stars are overlaid. For comparison, we also show the sample of δ Sct stars observed by *Kepler* (small orange points; Murphy et al. 2019).

[1] part of Scorpius was observed by *Kepler* K2 Mission and light curves for some bright stars have been made by Pope et al. (2019) using halo photometry.
[2] Pre-search Data Conditioning Simple Aperture Photometry
[3] `github.com/hvidy/tessbkgd`
[4] `github.com/hvidy/halophot`
[5] this list is maintained at `http://www.pas.rochester.edu/~emamajek/EEM_dwarf_UBVIJHK_colors_Teff.txt`

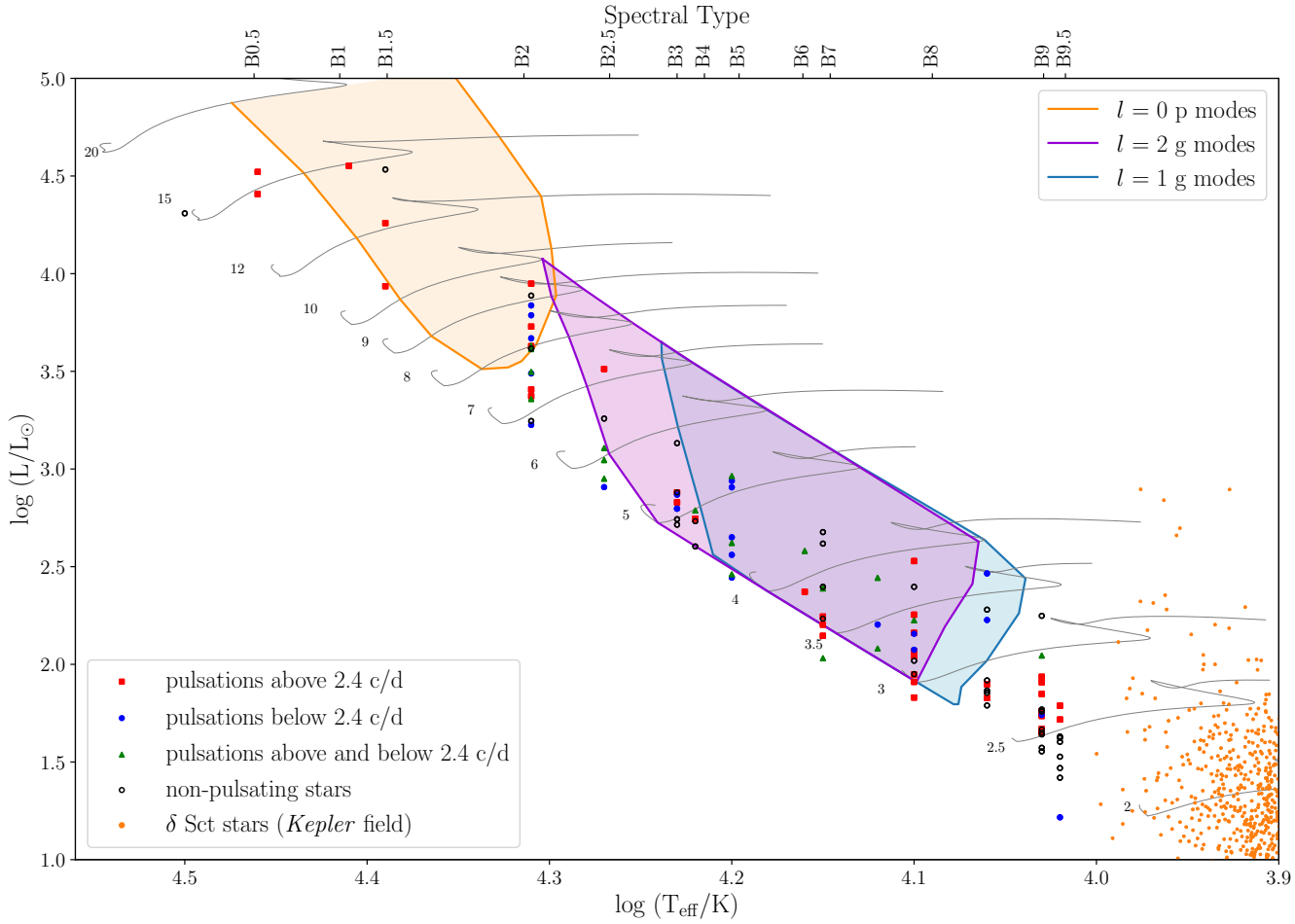

Figure 1. H–R diagram showing the variable stars in our Sco–Cen sample. Theoretical instability strips for $l = 0$ p modes and $l = 1$ and 2 g modes are shown in red, blue and purple. The small orange points show δ Sct stars observed by the *Kepler* Mission (Murphy et al. 2019).

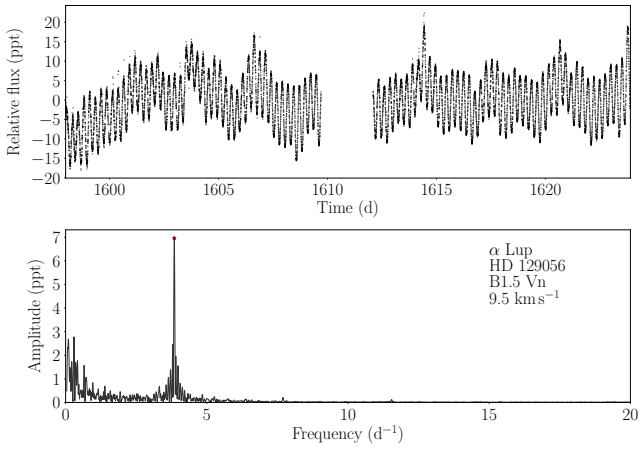

Figure 2. TESS light curve and Fourier amplitude spectra of α Lup (HD 129056; B1.5 Vn), which is a previously-known β Cep star (Nardetto et al. 2013).

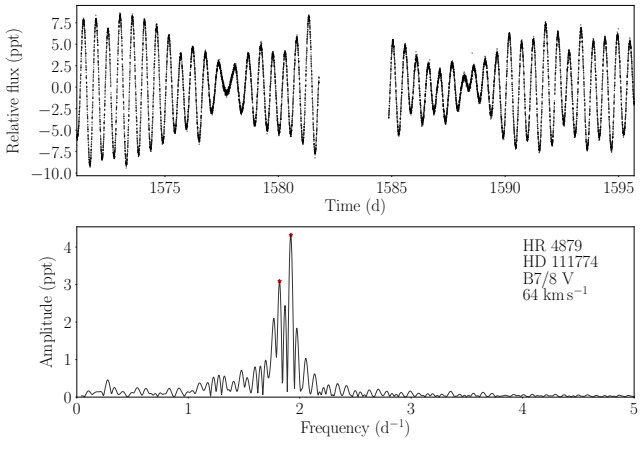

Figure 3. TESS light curve and Fourier amplitude spectra of HR 4879 (HD 111774; B7/8 V), an SPB star with two closely-spaced modes.

To assist the comparison with the theoretical instability strips for β Cep and SPB stars, we have indicated whether pulsations fall above or below a somewhat arbitrary threshold of 2.4 d^{-1}. We did not attempting a detailed frequency analysis. Instead, for each star that shows probable pulsations, we have listed up to four frequen-

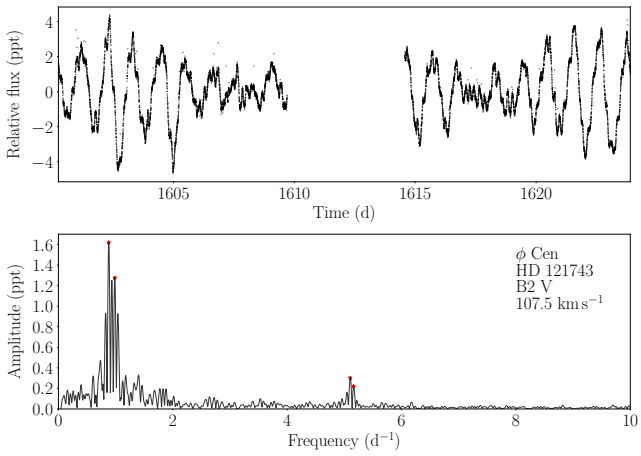

Figure 4. TESS light curve and Fourier amplitude spectra of ϕ Cen (HD 121743; B2 V), which is a hybrid pulsator (β Cep and SPB).

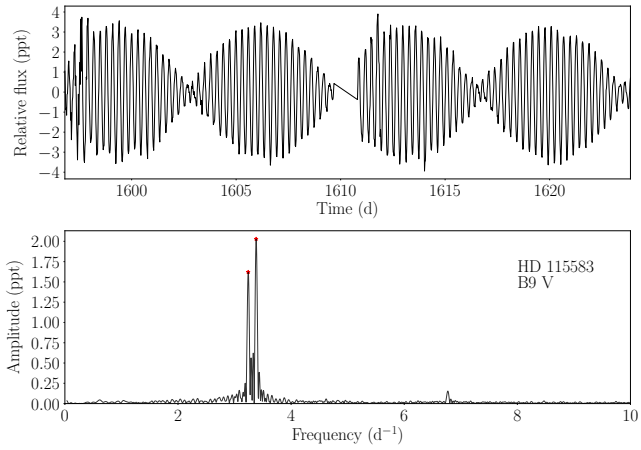

Figure 5. TESS light curve and Fourier amplitude spectra of HD 115583 (B9 V), which shows clear pulsations with two closely-spaced modes but is cooler that the standard SPB instability strip.

cies in Table 1. In particular, we list the two strongest pulsation peaks both above and below the 2.4-d^{-1} threshold (and excluding harmonics). We note that it can be difficult to distinguish between rotation and low-frequency pulsation in B stars (e.g., Briquet et al. 2007; Lee 2021), and it is possible that some stars listed as pulsating are actually rotational variables, and vice versa.

5 DISCUSSION

We see from Fig. 1 that pulsations occur across the full range of effective temperatures (see also Pedersen et al. 2019; Balona & Ozuyar 2020). They do not seem to correspond exactly with the theoretical instability strips, although we note that (i) some effective temperatures and luminosities could be in error, and (ii) the boundaries of the theoretical instability regions are sensitive to the heavy element abundance (Z), the opacity tables and rotation (e.g., Paxton et al. 2015; Moravveji 2016; Saio et al. 2017). In Fig. 6 we shows the pulsation frequencies listed in Table 1 as a function of effective temperature, with the symbols colour-coded by the $v \sin i$ of the star.

To decide whether the pulsations in a given star are p- or g-modes, it is helpful to know the mean density of the star. This is because the frequency of a particular p mode, such as the radial fundamental mode, scales from one star to another as the square root of the mean stellar density. Indeed, when plotting theoretical models it is common to scale the frequencies by dividing by $\sqrt{\rho}$ (e.g. Aerts et al. 2010). We show this for the observed pulsation frequencies in Figure 7, which is the same as Fig. 6 except that the frequencies have been divided by the square root of the stellar density. We made these rough density estimates for the stars in our sample as follows.

For each star, we estimated the radius using the Stefan–Boltzmann law ($L \propto R^2 {T_{\rm eff}}^4$), using the values in Table 1. We estimated masses from luminosities using a mass–luminosity relation (Eker et al. 2018), which we calibrated for Sco–Cen using published masses for 15 stars in our sample (Jang-Condell et al. 2015), as shown in Fig. 8. We found the relation to be

$$\frac{L}{\mathrm{L}_\odot} = 1.41 \left(\frac{M}{\mathrm{M}_\odot} \right)^{3.98} , \qquad (1)$$

which we used to estimate the masses for our sample.

The relationship between pulsation periods and mean density is usually written as (e.g., Catelan & Smith 2015, Sec. 5.2):

$$P = Q \left(\frac{\rho}{\rho_\odot} \right)^{-0.5} . \qquad (2)$$

The quantity Q, called the pulsation constant, depends on the pulsation mode. For example, Q is about 0.033 d for the fundamental radial mode in δ Sct stars (e.g., Breger 2000). It follows from Eq. 2 that the vertical axis in Fig. 7 shows $1/Q$, where Q is the pulsation constant (in days).

Stankov & Handler (2005) suggested that Q for β Cep stars peaks at 0.033 d (the same value as δ Sct stars), which corresponds to $1/Q = 30.0\,\mathrm{d}^{-1}$. To verify this, we used the grid of stellar models calculated by Stello et al. (2009) using the Aarhus stellar evolution code (ASTEC; Christensen-Dalsgaard 2008), and confirmed that the fundamental radial mode satisfies $1/Q = 30.2\,\mathrm{d}^{-1}$ across a range of masses and ages. In principle, all pulsations falling below this value cannot be p modes. However, we must remember that there are uncertainties in masses, both from uncertainties in luminosities and from scatter in the mass-luminosity relation (Fig. 8). An error of 0.2 in $\log M$, which is an extreme case, corresponds to a change of 0.1 in $\log(1/Q)$, which is a change of up to ~25% in $1/Q$.

We see in Fig. 7 that many of the pulsations in stars with spectral type B2 and cooler fall below the p-mode limit, which implies they must be g modes. In particular, this applies to the stars that lie between the accepted SPB and δ Sct instability strips (spectral types B9 and B9.5). The exception is μ Lup (B8 Ve), which is a Be star (Levenhagen & Leister 2006; Arcos et al. 2018) and so its anomalously high-frequency variations (18 and 33 d^{-1}) presumably come from oscillations in the circumstellar disk. As mentioned in the Introduction, there have been several reports of pulsations in B stars that are cooler than the standard range for SPB stars. Salmon et al. (2014) suggested the examples found by Mowlavi et al. (2013) in the young open cluster NGC 3766 are actually fast-rotating SPB pulsators, and this was endorsed by Saio et al. (2017). Looking at the $v \sin i$ values for our sample (colour-coded in Fig. 7), we indeed see that stars with spectral types B9 and B9.5 are indeed rotating rapidly ($v \sin i$ in the range 150 to 320 km s^{-1}).

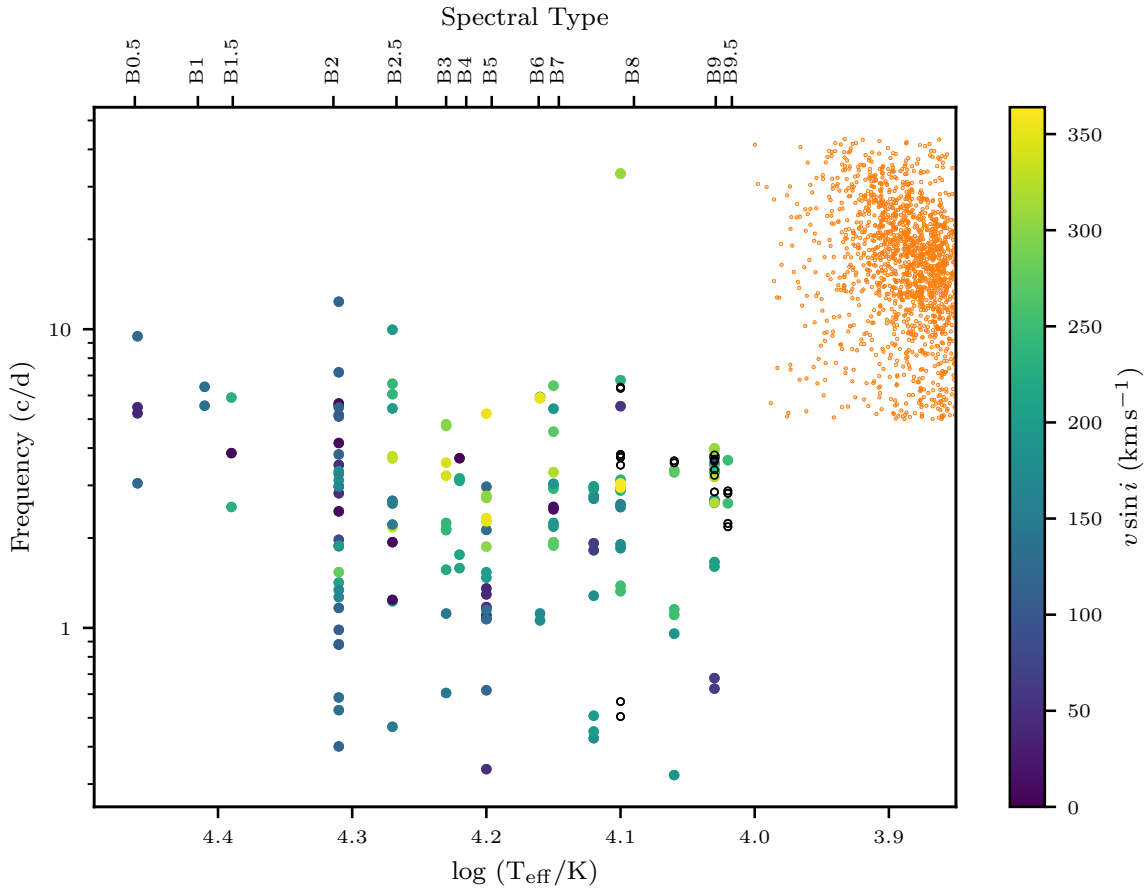

Figure 6. Pulsation frequencies of B stars in Sco–Cen from *TESS* observations, using the values listed in Table 1. Symbols are colour-coded with $v \sin i$, and left as open circles when this is not available. The small orange points show δ Sct stars observed by *Kepler* (Murphy et al. 2019).

5.1 Period–luminosity relations for fast rotators

Mowlavi et al. (2016) reported that the fast rotators in NGC 3766 followed two distinct period–luminosity (P–L) relations. Saio et al. (2017) suggested that these two relations corresponded to prograde sectoral g modes that are dipole ($l = m = 1$) and quadrupole ($l = m = 2$), respectively[6]. It is known that g-mode oscillations observed in a rapidly rotating stars are predominantly prograde sectoral modes (Van Reeth et al. 2016; Ouazzani et al. 2017; Pápics et al. 2017; Li et al. 2020). In such cases, the pulsation frequencies of g modes in the observer's frame are given as $\nu_{\rm obs} = \nu_{\rm corot} + m f_{\rm rot} \approx m f_{\rm rot}$. The latter relation is obtained assuming the frequencies of g modes in the co-rotating frame $\nu_{\rm corot}$ to be much smaller than the rotation frequency $f_{\rm rot}$; i.e., $\nu_{\rm corot} \ll m f_{\rm rot}$. In other words, these g modes in rapidly rotating stars should have periods similar to $P_{\rm rot}/m$.

Figure 1 shows that most SPB stars in the Sco–Cen association lie close to ZAMS, reflecting their very young ages. They are therefore expected to be rotating close to the critical rates. Assuming that they rotate at rates proportional to the critical rate of the ZAMS model corresponding to that luminosity, we can connect the rotation rate (and hence pulsation period $P_{\rm obs} \approx P_{\rm rot}/m$) with the luminosity as

$$\log(P_{\rm obs}/{\rm d}) \approx -\log(\Omega_{\rm rot}/\Omega_{\rm crit}) - 0.60 + 0.094(\log(L/{\rm L}_\odot) - 1.91) - \log(m). \quad (3)$$

Here, $\Omega_{\rm rot}/\Omega_{\rm crit}$ expresses the rotation frequency as a fraction of its critical value. Equation 3 represents a period–luminosity relation for given values of $\Omega_{\rm rot}/\Omega_{\rm crit}$ and m. The P–L relations for $m = 1$ and 2 with $\Omega_{\rm rot}/\Omega_{\rm crit} = 0.8$ are shown in Fig. 9 by dashed lines. Many of the rapidly rotating SPB stars fall approximately on these relations, lending support to our prediction. Furthermore, this figure shows that variable stars cooler and fainter ($\sim 1.5 < \log(L/L_\odot) \approx 2.0$) than the standard SPB instability boundary (Fig. 1) fall approximately on the $m = 1$ P–L relation, indicating they are rapidly rotating SPB stars (g-mode pulsators).

The PL relations for rapidly rotating SPB stars in the Sco-Cen association we found are the same type as the relations for rapidly rotating SPB stars in the young open cluster NGC 3766 found by Mowlavi et al. (2016) and modeled by Saio et al. (2017). The presence of such P–L relations in the young cluster and the OB association indicates many newly born B-type (single) stars rotate nearly critically.

[6] we adopt the convention that prograde modes have $m > 0$

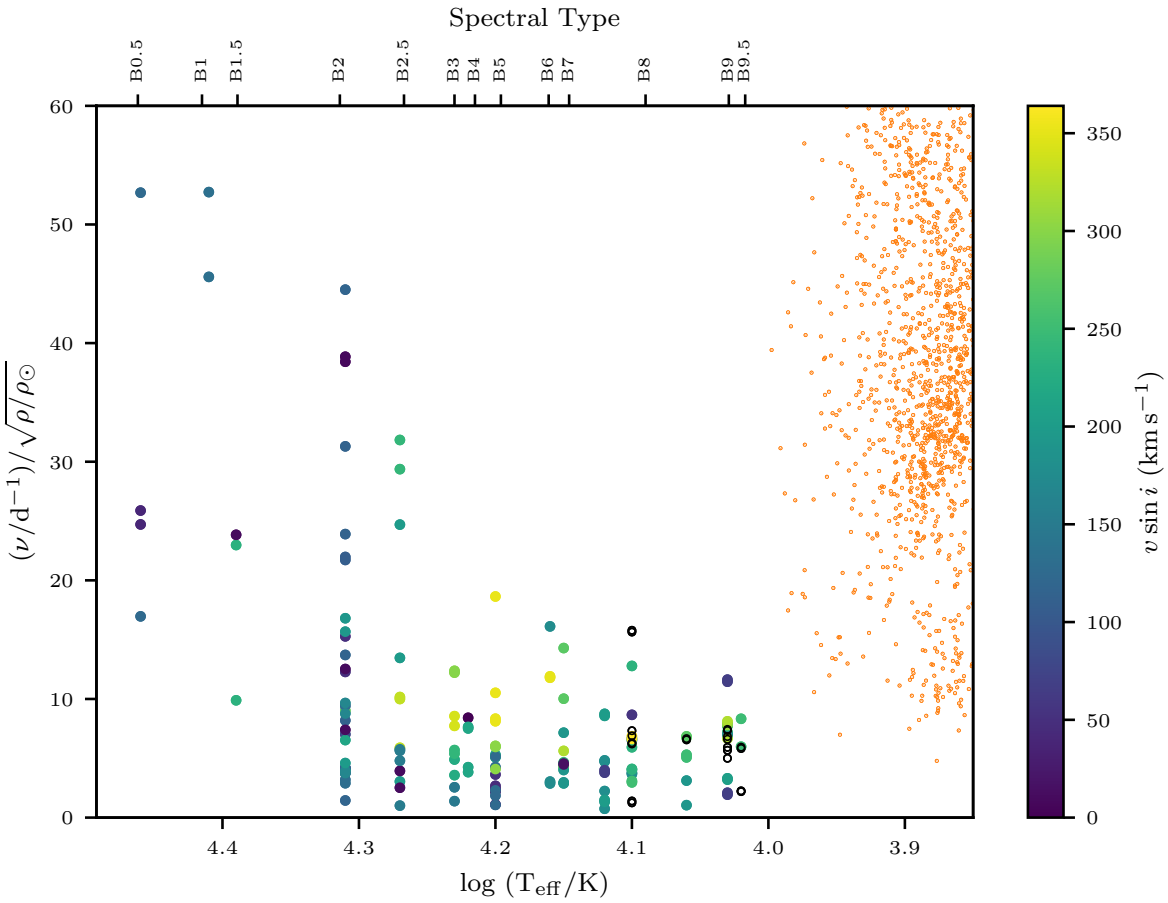

Figure 7. Scaled pulsation frequencies as a function of stellar effective temperature. Similar to Fig. 6 except that the frequencies have been divided by the square root of the mean stellar density (see text). Densities for the *Kepler* δ Sct stars (small orange points) were calculated using masses and radii from Murphy et al. (2019).

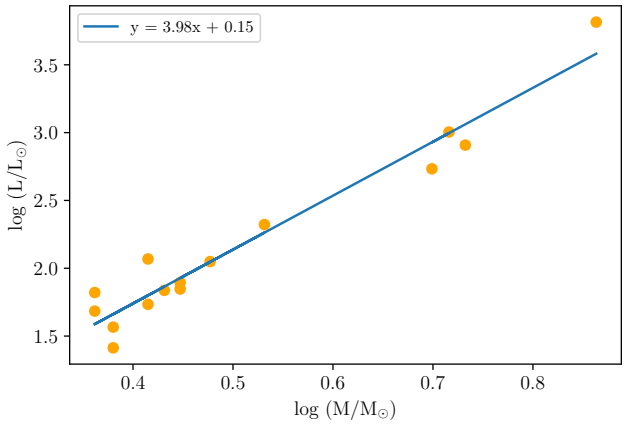

Figure 8. Mass–luminosity relationship used to estimate masses of stars in our sample.

6 NOTES ON INDIVIDUAL STARS

6.1 α Crucis: a new β Cephei star

The brightest star in the Southern Cross is a multiple system whose two most luminous components are α^1 Cru (HD 108248; B0.5 V; $V = 1.28$) and α^2 Cru (HD 108249; B1 V; $V = 1.58$). They are separated by only 4″ and so the *TESS* light curve includes both (*TESS* pixels are 21″). As described in Sec. 2, the extreme brightness of this target required us to use a pixel-level analysis to extract the light curve.

There are no previous reports of photometric variability in α Cru but our *TESS* light curve (Fig. 10) clearly shows low-amplitude pulsations, making it the second-brightest β Cep star in the sky (after β Cen). The amplitude spectrum shows modes at frequencies 3.048 d^{-1} (amplitude 0.25 ppt), 9.468 d^{-1} (0.21 ppt), 15.548 d^{-1} (0.05 ppt) and 9.854 d^{-1} (0.03 ppt), as well as peaks at combination frequencies of the two strongest modes. It is not possible to tell definitively whether the pulsations detected by *TESS* occur in α^1 Cru or α^2 Cru (or both), although the presence of combination frequencies shows that the two strongest modes must both occur in the same star. For the figures in this paper, we used the parameters of α^1 Cru.

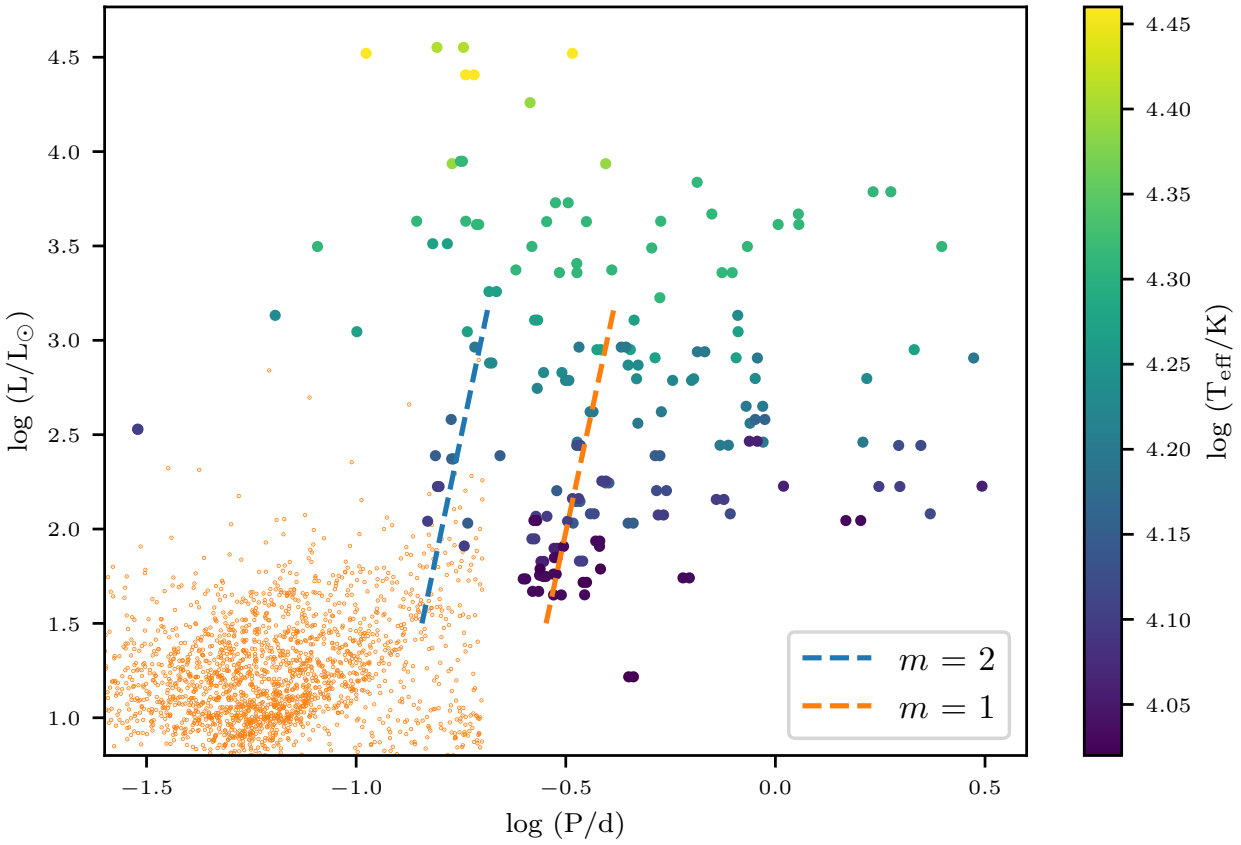

Figure 9. Period–luminosity diagram for the stars in our Sco–Cen sample (colour-coded with effective temperature), as well as δ Sct stars observed by *Kepler* (orange points; Murphy et al. 2019. Dashed lines show theoretical P–L relations for sectoral g modes for a rotation rate of 0.8 times the critical value (see Sec. 5.1).

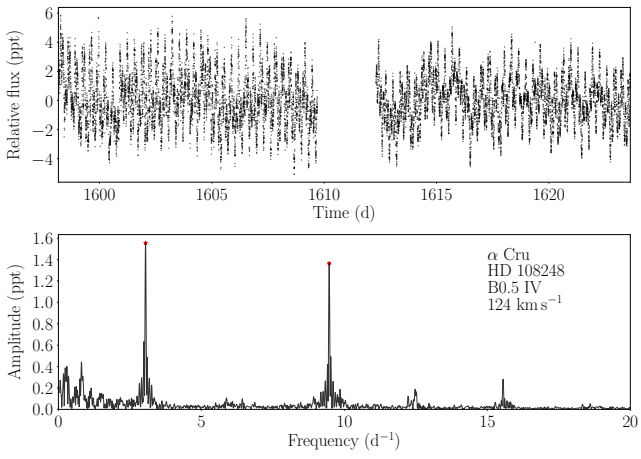

Figure 10. *TESS* light curve and amplitude spectrum of the β Cep star α Cru (see Sec. 6.1).

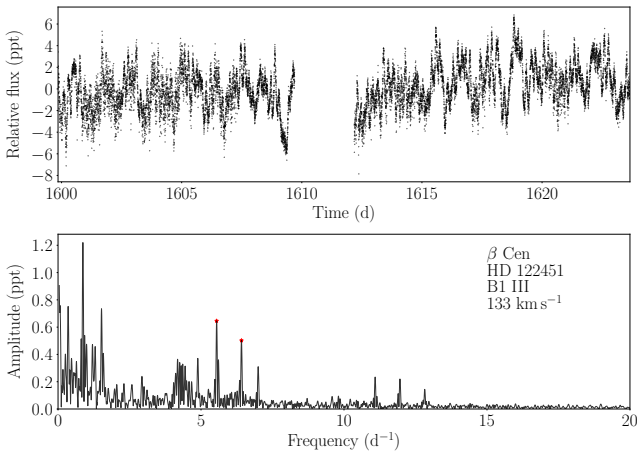

Figure 11. *TESS* light curve and amplitude spectrum of the β Cep star β Cen (see Sec. 6.2).

6.2 β Centaurus: a β Cephei star with possible rotationally-split modes

β Cen (HD 122451; B1 III) is known to show multi-periodic pulsations, based on photometry spanning 146 d from the BRITE-Constellation (Pigulski et al. 2016). It is an interferometric and double-lined spectroscopic binary with two nearly-equal components (Robertson et al. 1999; Ausseloos et al. 2006), and our luminosity is calculated from an absolute magnitude for the primary of $M_V = -4.03$ (Pigulski et al. 2016). Our *TESS* light curve, extracted from pixel-level data (Sec. 2), confirms a rich spectrum of pulsation modes, including some that were not detected with BRITE (the

BRITE spacecraft are in low-Earth orbit, which results in an effective Nyquist frequency of 7.17 d^{-1} (see Pigulski et al. 2016). The TESS amplitude spectrum appears to show rotational triplets and clearly deserves more detailed study.

6.3 ξ^2 Cen: a hybrid pulsator with regular spacings

The light curve for ξ^2 Cen (HD 113791; B3) shows both g and p modes (Fig. 12). The g modes appear to have a regular structure that has a similar spacing to other SPB stars (Pápics et al. 2017; Aerts 2021; Szewczuk et al. 2021). Remarkably, we also see a regular pattern of p modes in ξ^2 Cen (top panel of Fig. 12). Such regularity is common in solar-like oscillators (Chaplin & Miglio 2013) and also occurs in young δ Sct stars (Bedding et al. 2020), but is very unusual in β Cep stars. One exception is V1449 Aql (HD 180642), for which CoRoT observations showed evidence for a large frequency spacing of $\Delta\nu = 2.3\,d^{-1}$ (Belkacem et al. 2009). In ξ^2 Cen, the spacing between the peaks yields a large frequency spacing of $\Delta\nu = 3.46\,d^{-1}$. Using the standard scaling relation that $\Delta\nu$ scales approximately with the square root of density (e.g. Aerts et al. 2010), this implies a mean stellar density of 0.087 in solar units. This is in reasonable agreement with the rough estimate of 0.073 that we made in Sec. 5. It is also interesting that the p modes peaks are broadened, possibly indicating damping similar to that seen in V1449 Aql (Belkacem et al. 2009, 2010). The bottom panel of Fig. 12 shows the amplitude spectrum in échelle format, after first removing low-frequency variations with a high-pass filter. The pattern with two clear ridges is very reminiscent of those seen in young δ Sct stars (Bedding et al. 2020). This star is clearly worthy of further study.

6.4 HD 132094: a short-period heartbeat star

The star HD 132094 (spectral type B9) was not previously known to be a binary. However, its *TESS* light curve (Fig. 13) shows it is a member of the class of eccentric binaries with tidal distortions (so-called heartbeat stars) that were discovered in large numbers by the *Kepler* Mission (e.g., Thompson et al. 2012; Kirk et al. 2016). The period is 0.586 d, which appears to be the shortest among previously published heartbeat stars (Kirk et al. 2016; Kołaczek-Szymański et al. 2021). The phase-folded light curve shows evidence for tidally-forced pulsations (not included in Table 1) and this star certainly deserves further study.

6.5 τ Lib: a heartbeat star with pulsations

The star τ Lib (HD 139365; B2.5) is known to be a spectroscopic binary, and photometry with the BRITE mission showed it to be a heartbeat star with a period of 3.41 d (Pigulski et al. 2018). This is confirmed by the *TESS* light curve from Sector 38, which gives an orbital frequency of 0.290 d^{-1} and also shows clear pulsations (Fig. 14). The two strongest pulsation peaks are listed in Table 1, and we note that f_1 coincides with 16 times the orbital frequency.

6.6 π Lup: an eclipsing binary with pulsations

π Lup (HR 5605; HD 133242; B5 V) is a multiple system with at least four components (Nitschelm 2004) but not previously known to be eclipsing. The *TESS* light curve (Fig. 15) shows two narrow eclipses with depths of 1% and separated by 15.50 d. The amplitude spectrum (shown in Fig. 15 after removal of the eclipses) shows

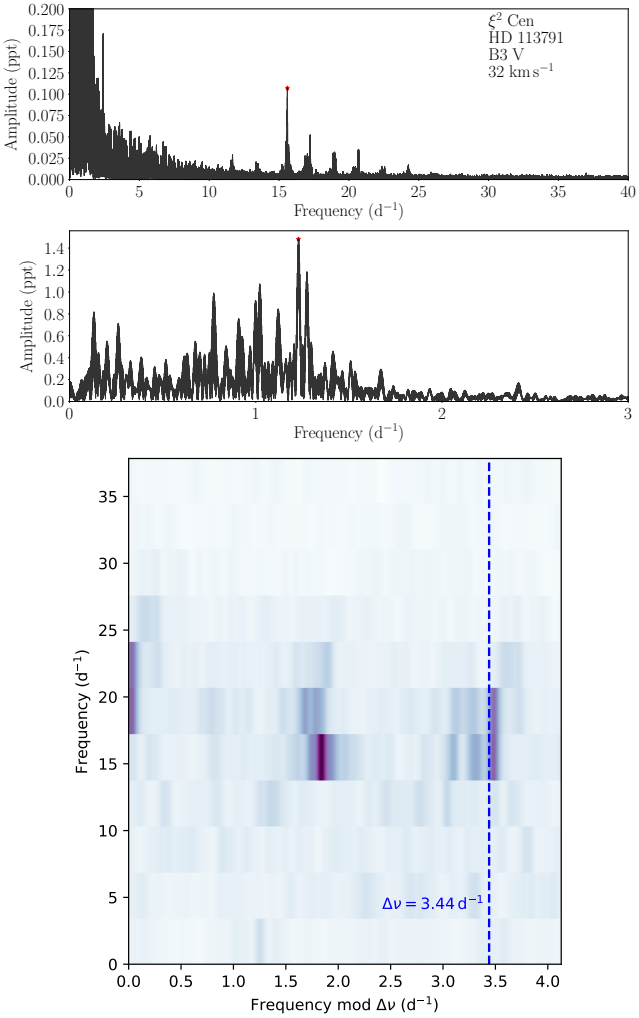

Figure 12. *TESS* amplitude spectrum of the hybrid pulsator ξ^2 Cen from *TESS* Sectors 11, 37 and 38, showing the regions with p modes (top panel) and g modes (middle panel). We also show the amplitude spectrum in échelle format (bottom panel) after first removing low-frequency variations (see Sec. 6.3).

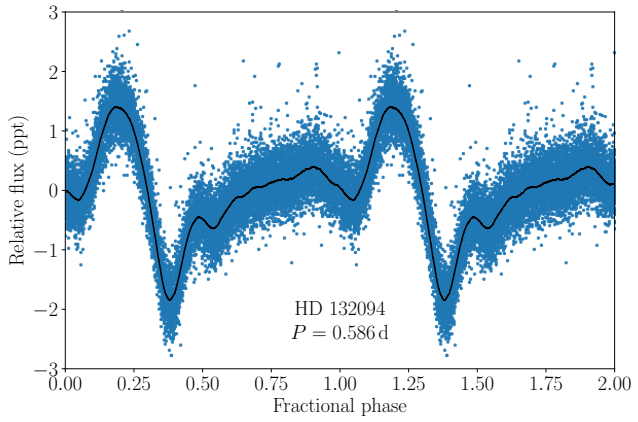

Figure 13. Light curve of the heartbeat star HD 132094, folded at the orbital period.

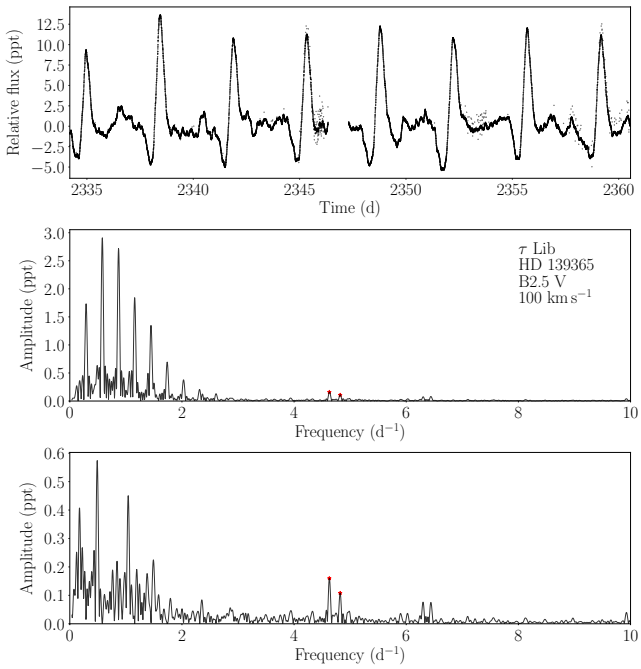

Figure 14. *TESS* Light curve of τ Lib.The top panel is original light curve, the middle panel is the Fourier Transform of the original light curve, and the bottom panel is the Fourier Transform of the light curve after removing the first 9 harmonics of the orbital frequency.

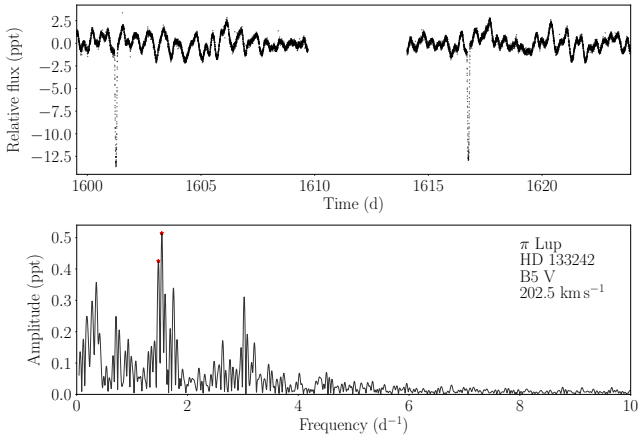

Figure 15. *TESS* observations of π Lup (B5 V) from Sector 11. The light curve (upper panel) shows it to be an eclipsing binary with pulsations. The amplitude spectrum after removing the eclipses (lower panel) shows pulsations.

peaks at 1.5 d^{-1} that are consistent with SPB pulsations, or possibly r modes.

6.7 HR 5846: an eclipsing binary with tidally-forced pulsations

HR 5846 (HD 140285; A0 V). This star not in our sample because it does not have B spectral type but we mention it here because of its interesting light curve. The *TESS* data (Fig. 16) shows detached eclipses (period 2.1 d) as well as pulsations at exactly 10 times

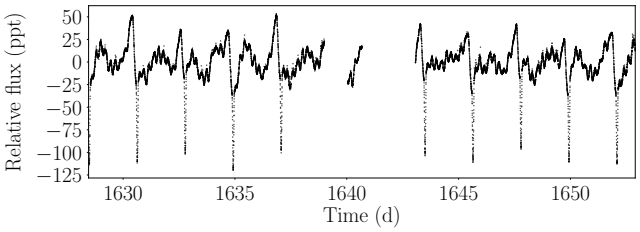

Figure 16. *TESS* light curve of the star HR 5846 (A0 V), showing eclipses and tidally forced pulsations.

the orbital frequency. These are presumably tidally forced g modes and have an unusually large amplitude (almost 1%). Note that x-ray emission from HR 5846 was reported by Motch et al. (1997).

6.8 Other eclipsing and close binaries

Light curves for the following stars are shown in the on-line supplementary material:

- μ^1 Sco (HD 151890; B1.5 +B) is known to be a semi-detached eclipsing binary with a period of 1.45 d (van Antwerpen & Moon 2010). This is confirmed by the *TESS* light curve, which shows no sign of pulsations after prewhitening with the first 12 harmonics of the orbital frequency.
- V964 Cen (HD 115823; B5) is catalogued as a short-period detached eclipsing binary (Samus' et al. 2017) but the *TESS* light curve clearly shows it is actually an SPB star.
- V831 Cen (HD 114529; B7) is known to be a close binary (ellipsoidal variable) with a period of 0.642 d (Budding et al. 2010), which is confirmed by the *TESS* light curve.
- GG Lup (HD 135876; B7) is known to be a detached eclipsing binary with a period of 1.85 d (e.g., Budding et al. 2015). This is confirmed by the *TESS* light curve, which also shows low-amplitude variability outside of the eclipses (around 1.6 d^{-1}) that may indicate tidally-forced pulsations.
- HR 4913 (HD 112409; V945 Cen; B8/9 V) is known to be a close binary (ellipsoidal variable) with a period 0.65 d (Harmanec et al. 2010), which is confirmed by the *TESS* light curve.

6.9 Other stars

These stars are ordered by spectral type:

- τ Sco (HD 149438; B0 V) is not catalogued as a β Cep star and no line profile variations have been reported (Telting et al. 2006). The TESS light curve shows no evidence for variability and we can rule out β Cep pulsations down to a level of about 50 ppm.
- β Cru (HD 111123; B0.5 III) is known to be a multi-periodic β Cep star, which is confirmed by the *TESS* light curve. Aerts et al. (1998) found it to be a spectroscopic binary in an eccentric 5-yr orbit, in which the primary (B0.5 III) is the β Cep variable and the secondary is a B2 V star. The strongest modes in the *TESS* data have frequencies of 5.230, 5.487, 5.969, and 3.529 d^{-1}, which agree with those found by Cuypers et al. (2002) using photometry spanning 17 d from the star tracker on the *WIRE* satellite. The *TESS* light curve from Sector 11 for this star has been analysed in detail by Cotton et al. (2021).
- α Lup (HD 129056; B1.5 Vn) is known to be a single-mode β Cep star (Lampens & Goossens 1982; Mathias et al. 1994;

Nardetto et al. 2013). The *TESS* light curve confirms the mode at 3.848 d^{-1} (7.0 ppt), and subtracting this mode shows much weaker peaks (0.6–0.7 ppt) at 3.318, 3.916 and 3.976 d^{-1}.

- ν Cen (HD 120307; B2) This system is a spectroscopic binary with an orbital period of 2.625 d. The TESS 2-minute data curve shows variations that matches the orbital period. After prewhitening this period, there is some irregular variability but no evidence for coherent pulsations.
- γ Lup (HD 138690; B2 IV; $V = 2.77$) This is a visual binary with nearly equal components separated by about half an arcsecond (Herschel 1847). One of the components is a spectroscopic binary with an orbital period of 2.625 d. It was not previously reported as a β Cep star. The TESS 2-minute light curve shows variations that matches the orbital period. After prewhitening this period, the light curve appears to show several low-amplitude peaks in the range 1.5 to 15 d^{-1} that may indicate SPB and β Cep pulsations, but these are not listed in the table.

7 CONCLUSIONS

We have examined the light curves of 119 B-type stars in the Sco–Cen Association that have been observed by *TESS*. Pulsations are seen in 80 stars, covering the whole spectral range in the H–R diagram. In particular, we confirm the presence of low-frequency pulsations in stars whose effective temperatures lie between those normally associated with SPB and δ Sct stars. By taking the stellar densities into account, we conclude that these cannot be p modes and confirm previous suggestions that these are probably rapidly-rotating SPB stars. We also confirm that they follow two period–luminosity relations that are consistent with prograde sectoral g modes that are dipole ($l = m = 1$) and quadrupole ($l = m = 2$), respectively.

One of the stars (ξ^2 Cen; Sec. 6.3) is a hybrid pulsator that shows regular spacings in both g and p modes. In particular, the p modes show a remarkable regularity that is reminiscent of solar-like oscillations. Our sample also includes several interesting binaries, including a very short-period heartbeat star (HD 132094; Sec. 6.4), a previously unknown eclipsing binary (π Lup; Sec 6.6), and an eclipsing binary with high-amplitude tidally driven pulsations (HR 5846; Sec. 6.7). Overall, the results show the power of *TESS* for studying variability in bright stars.

ACKNOWLEDGEMENTS

We thank Mike Ireland and Aaron Rizzuto for helpful discussions. We gratefully acknowledge support from the Australian Research Council through Discovery Project DP210103119, and from the Danish National Research Foundation (Grant DNRF106) through its funding for the Stellar Astrophysics Center (SAC). We are grateful to the entire *TESS* team for providing the data used in this paper. This work made use of several publicly available `python` packages: `astropy` (Astropy Collaboration 2013, 2018), `echelle` (Hey & Ball 2020), `lightkurve` (Lightkurve Collaboration 2018), `matplotlib` (Hunter 2007), `numpy` (Harris et al. 2020), and `scipy` (Virtanen et al. 2020).

REFERENCES

Aerts C., 2021, Reviews of Modern Physics, 93, 015001
Aerts C., Kolenberg K., 2005, A&A, 431, 615
Aerts C., De Cat P., Cuypers J., Becker S. R., Mathias P., De Mey K., Gillet D., Waelkens C., 1998, A&A, 329, 137
Aerts C., Christensen-Dalsgaard J., Kurtz D. W., 2010, Asteroseismology. Springer
Aerts C., Simón-Díaz S., Groot P. J., Degroote P., 2014, A&A, 569, A118
Arcos C., Kanaan S., Chávez J., Vanzi L., Araya I., Curé M., 2018, MNRAS, 474, 5287
Astropy Collaboration 2013, A&A, 558, A33
Astropy Collaboration 2018, AJ, 156, 123
Ausseloos M., Aerts C., Lefever K., Davis J., Harmanec P., 2006, A&A, 455, 259
Balona L. A., Feast M. W., 1975, MNRAS, 172, 191
Balona L. A., Ozuyar D., 2020, MNRAS, 493, 5871
Balona L. A., Baran A. S., Daszyńska-Daszkiewicz J., De Cat P., 2015, MNRAS, 451, 1445
Balona L. A., et al., 2016, MNRAS, 460, 1318
Balona L. A., et al., 2019, MNRAS, 485, 3457
Bedding T. R., et al., 2020, Nature, 581, 147
Belkacem K., et al., 2009, Science, 324, 1540
Belkacem K., Dupret M. A., Noels A., 2010, A&A, 510, A6
Blaauw A., 1946, Publications of the Kapteyn Astronomical Laboratory Groningen, 52, 1
Bowman D. M., 2020, Frontiers in Astronomy and Space Sciences, 7, 70
Breger M., 2000, in ASP Conf. Series, Vol. 210. p. 3
Briquet M., Hubrig S., De Cat P., Aerts C., North P., Schöller M., 2007, A&A, 466, 269
Brown A. G. A., Verschueren W., 1997, A&A, 319, 811
Budding E., Erdem A., Inlek G., Demircan O., 2010, MNRAS, 403, 1448
Budding E., Butland R., Blackford M., 2015, MNRAS, 448, 3784
Burssens S., et al., 2020, arXiv e-prints, p. arXiv:2005.09658
Catelan M., Smith H. A., 2015, Pulsating Stars. Wiley-VCH
Chaplin W. J., Miglio A., 2013, Annual Review of Astronomy and Astrophysics, 51, 353
Christensen-Dalsgaard J., 2008, Ap&SS, 316, 13
Cotton D., et al., 2021, Nature Astronomy, in press
Cuypers J., Aerts C., Buzasi D., Catanzarite J., Conrow T., Laher R., 2002, A&A, 392, 599
Daszyńska-Daszkiewicz J., Pamyatnykh A. A., Walczak P., Colgan J., Fontes C. J., Kilcrease D. P., 2017, MNRAS, 466, 2284
Daszyńska-Daszkiewicz J., Walczak P., Pamyatnykh A., Szewczuk W., 2020, in Małek K., Polińska M., Majczyna A., Stachowski G., Poleski R., Wyrzykowski Ł., óżańska A., eds, Proceedings of the Polish Astronomical Society Vol. 10, XXXIX Polish Astronomical Society Meeting. pp 136–141 (`arXiv:1912.00409`)
De Cat P., Uytterhoeven K., Gutiérrez-Soto J., Degroote P., Simón-Díaz S., 2011, in Neiner C., Wade G., Meynet G., Peters G., eds, IAU Symposium Vol. 272, Active OB Stars: Structure, Evolution, Mass Loss, and Critical Limits. pp 433–444, doi:10.1017/S1743921311011070
De Zeeuw P. T., Hoogerwerf R., de Bruijne J. H. J., Brown A. G. A., Blaauw A., 1999, AJ, 117, 354
Degroote P., et al., 2009, A&A, 506, 471
Degroote P., et al., 2010, Nature, 464, 259
Dziembowski W. A., Pamiatnykh A. A., 1993, MNRAS, 262, 204
Dziembowski W. A., Moskalik P., Pamyatnykh A. A., 1993, MNRAS, 265, 588
Eker Z., et al., 2018, MNRAS, 479, 5491
Gautschy A., Saio H., 1993, MNRAS, 262, 213
Handler G., et al., 2007, Communications in Asteroseismology, 150, 193
Handler G., et al., 2008, Communications in Asteroseismology, 157, 315
Harmanec P., Aerts C., Prša A., Verhoelst T., Kolenberg K., 2010, A&A, 520, A73
Harris C. R., et al., 2020, Nature, 585, 357
Herschel J. F. W., 1847, Results of astronomical observations made during the years 1834, 5, 6, 7, 8, at the Cape of Good Hope; being the completion of a telescopic survey of the whole surface of the visible heavens, commenced in 1825. Smith, Elder and Co, London
Hey D. R., Ball W. H., 2020, Echelle: Dynamic echelle diagrams for

asteroseismology, doi:10.5281/zenodo.3629933, https://doi.org/10.5281/zenodo.3629933
Houk N., 1978, Michigan catalogue of two-dimensional spectral types for the HD stars. Univ. Michigan, Ann Arbor
Houk N., 1982, Michigan Catalogue of Two-dimensional Spectral Types for the HD stars. Volume_3. Declinations -40_*f*0 to -26_*f*0.. Univ. Michigan, Ann Arbor
Houk N., Cowley A. P., 1975, University of Michigan Catalogue of two-dimensional spectral types for the HD stars. Volume I. Declinations -90_ to -53_*f*0.. Univ. Michigan, Ann Arbor
Houk N., Smith-Moore M., 1988, Michigan Catalogue of Two-dimensional Spectral Types for the HD Stars. Volume 4, Declinations -26°.0 to -12°.0.. Univ. Michigan, Ann Arbor
Houk N., Swift C., 1999, Michigan catalogue of two-dimensional spectral types for the HD Stars. Volume 5. Univ. Michigan, Ann Arbor
Huang C. X., et al., 2020, Research Notes of the American Astronomical Society, 4, 204
Hunter J. D., 2007, Computing in Science & Engineering, 9, 90
Jang-Condell H., Chen C. H., Mittal T., Manoj P., Watson D., Lisse C. M., Nesvold E., Kuchner M., 2015, ApJ, 808, 167
Jones D. H. P., Shobbrook R. R., 1974, MNRAS, 166, 649
Kirk B., et al., 2016, AJ, 151, 68
Kołaczek-Szymański P. A., Pigulski A., Michalska G., Moździerski D., Różański T., 2021, A&A, 647, A12
Lampens P., Goossens M., 1982, A&A, 115, 413
Lata S., Yadav R. K., Pandey A. K., Richichi A., Eswaraiah C., Kumar B., Kappelmann N., Sharma S., 2014, MNRAS, 442, 273
Lee U., 2021, arXiv e-prints, p. arXiv:2105.06667
Lenz P., 2011, in New Horizons in Astronomy. p. 3
Levenhagen R. S., Leister N. V., 2006, MNRAS, 371, 252
Li G., Van Reeth T., Bedding T. R., Murphy S. J., Antoci V., Ouazzani R.-M., Barbara N. H., 2020, MNRAS, 491, 3586
Lightkurve Collaboration 2018, Lightkurve: Kepler and TESS time series analysis in Python, Astrophysics Source Code Library (ascl:1812.013)
Majewska-Świerzbinowicz A., Pigulski A., Szabó R., Csubry Z., 2008, in Journal of Physics Conference Series. p. 012068 (arXiv:0711.1627), doi:10.1088/1742-6596/118/1/012068
Mathias P., Aerts C., de Pauw M., Gillet D., Waelkens C., 1994, A&A, 283, 813
Moravveji E., 2016, MNRAS, 455, L67
Motch C., Haberl F., Dennerl K., Pakull M., Janot-Pacheco E., 1997, A&A, 323, 853
Mowlavi N., Barblan F., Saesen S., Eyer L., 2013, A&A, 554, A108
Mowlavi N., Saesen S., Semaan T., Eggenberger P., Barblan F., Eyer L., Ekström S., Georgy C., 2016, A&A, 595, L1
Moździerski D., Pigulski A., Kopacki G., Kołaczkowski Z., Stęślicki M., 2014, Acta Astron., 64, 89
Moździerski D., et al., 2019, A&A, 632, A95
Murphy S. J., Hey D., Van Reeth T., Bedding T. R., 2019, MNRAS, 485, 2380
Murphy S. J., Joyce M., Bedding T. R., White T. R., Kama M., 2021, MNRAS, 502, 1633
Nardetto N., Mathias P., Fokin A., Chapellier E., Pietrzynski G., Gieren W., Graczyk D., Mourard D., 2013, A&A, 553, A112
Nitschelm C., 2004, in Hilditch R. W., Hensberge H., Pavlovski K., eds, Astronomical Society of the Pacific Conference Series Vol. 318, Spectroscopically and Spatially Resolving the Components of the Close Binary Stars. pp 291–293
Ouazzani R.-M., Salmon S. J. A. J., Antoci V., Bedding T. R., Murphy S. J., Roxburgh I. W., 2017, MNRAS, 465, 2294
Pápics P. I., et al., 2017, A&A, 598, A74
Paxton B., Bildsten L., Dotter A., Herwig F., Lesaffre P., Timmes F., 2011, ApJS, 192, 3
Paxton B., et al., 2013, ApJS, 208, 4
Paxton B., et al., 2015, ApJS, 220, 15
Pecaut M. J., Mamajek E. E., 2013, ApJS, 208, 9
Pecaut M. J., Mamajek E. E., 2016, MNRAS, 461, 794
Pedersen M. G., et al., 2019, ApJ, 872, L9
Pedersen M. G., et al., 2021, Nature Astronomy,
Pigulski A., et al., 2016, A&A, 588, A55
Pigulski A., et al., 2018, in Wade G. A., Baade D., Guzik J. A., Smolec R., eds, 3rd BRITE Science Conference. pp 115–117
Pope B. J. S., et al., 2019, ApJS, 245, 8
Preibisch T., Mamajek E., 2008, in Reipurth B., ed., ASP Monograph Publications Vol. 5, Handbook of Star Forming Regions, Volume II. Astron. Soc. Pacific, p. 235
Ricker G. R., et al., 2015, J. Astron. Telescopes, Instruments, and Systems, 1, 014003
Rizzuto A. C., Ireland M. J., Robertson J. G., 2011, MNRAS, 416, 3108
Rizzuto A. C., et al., 2013, MNRAS, 436, 1694
Robertson J. G., Bedding T. R., Aerts C., Waelkens C., Marson R. G., Barton J. R., 1999, MNRAS, 302, 245
Saesen S., et al., 2010, A&A, 515, A16
Saesen S., Briquet M., Aerts C., Miglio A., Carrier F., 2013, AJ, 146, 102
Saio H., Cox J. P., 1980, ApJ, 236, 549
Saio H., Winget D. E., Robinson E. L., 1983, ApJ, 265, 982
Saio H., Ekström S., Mowlavi N., Georgy C., Saesen S., Eggenberger P., Semaan T., Salmon S. J. A. J., 2017, MNRAS, 467, 3864
Salmon S., Montalbán J., Morel T., Miglio A., Dupret M. A., Noels A., 2012, MNRAS, 422, 3460
Salmon S. J. A. J., Montalbán J., Reese D. R., Dupret M. A., Eggenberger P., 2014, A&A, 569, A18
Samus' N. N., Kazarovets E. V., Durlevich O. V., Kireeva N. N., Pastukhova E. N., 2017, Astronomy Reports, 61, 80
Stankov A., Handler G., 2005, ApJS, 158, 193
Stello D., et al., 2009, ApJ, 700, 1589
Szewczuk W., Walczak P., Daszyńska-Daszkiewicz J., 2021, MNRAS, 503, 5894
Telting J. H., Schrijvers C., Ilyin I. V., Uytterhoeven K., De Ridder J., Aerts C., Henrichs H. F., 2006, A&A, 452, 945
Thompson S. E., et al., 2012, ApJ, 753, 86
Thoul A., 2009, Communications in Asteroseismology, 159, 35
Van Reeth T., Tkachenko A., Aerts C., 2016, A&A, 593, A120
Virtanen P., et al., 2020, Nature Methods, 17, 261
Waelkens C., 1991, A&A, 246, 453
White T. R., et al., 2017, MNRAS, 471, 2882
Wolff S. C., Strom S. E., Dror D., Venn K., 2007, AJ, 133, 1092
Zorec J., Royer F., 2012, A&A, 537, A120
de Geus E. J., de Zeeuw P. T., Lub J., 1989, A&A, 216, 44
van Antwerpen C., Moon T., 2010, MNRAS, 401, 2059
van Heerden P., Engelbrecht C. A., Martinez P., 2020, MNRAS, 492, 4635

Table 1: Sample of B stars in Sco–Cen that have been observed by *TESS* (ordered by spectral type).

Name	HD	HIP	V	Sp. type	$\log(T_{\rm eff}/{\rm K})$	$\log(L/{\rm L}_\odot)$	$v \sin i$ (km s^{-1})	f_1 (d^{-1})	f_2 (d^{-1})	f_3 (d^{-1})	f_4 (d^{-1})
τ Sco	149438	81266	2.81	B0 V	4.50	4.31	8.0	—	—	—	—
β Cru	111123	62434	1.25	B0.5 III	4.46	4.41	39.5	5.23	5.48	—	—
α Cru	108248	60718	1.28	B0.5 IV	4.46	4.52	124.0	3.05	9.47	—	—
β Cen	122451	68702	0.58	B1 III	4.41	4.55	133.0	5.55	6.41	—	—
δ Lup	136298	75141	3.19	B1.5 IV	4.39	3.94	232.5	5.90	2.54	—	—
μ^1 Sco	151890	82514	2.98	B1.5 IV + B	4.39	4.53	180.0	—	—	—	—
α Lup	129056	71860	2.29	B1.5 Vn	4.39	4.26	9.5	3.85	—	—	—
HR 6143	148703	80911	4.23	B2 III-IV	4.31	3.49	81.5	—	—	1.97	—
τ^1 Lup	126341	70574	4.55	B2 IV	4.31	3.95	7.5	5.64	5.58	—	—
α Mus	109668	61585	2.65	B2 IV	4.31	3.63	114.0	7.17	5.48	1.88	—
β Lup	132058	73273	2.68	B2 IV	4.31	3.79	130.0	—	—	0.53	0.58
δ Cru	106490	59747	2.75	B2 IV	4.31	3.67	214.0	—	—	0.88	1.42
κ Cen	132200	73334	3.11	B2 IV	4.31	3.62	20.0	—	—	—	—
ν Cen	120307	67464	3.39	B2 IV	4.31	3.62	92.0	—	—	—	—
γ Lup	138690	76297	2.76	B2 IV	4.31	3.84	276.5	—	—	1.54	—
μ^2 Sco	151985	82545	3.54	B2 IV	4.31	3.63	49.0	2.82	3.51	—	—
υ^1 Cen	121790	68282	3.87	B2 IV/V	4.31	3.41	124.0	2.98	—	—	—
ρ Sco	142669	78104	3.86	B2 IV/V	4.31	3.50	117.0	3.81	12.37	0.40	1.17
μ Cen	120324	67472	3.43	B2 IV/Vne	4.31	3.73	192.5	3.35	3.12	—	—
χ Cen	122980	68862	4.34	B2 V	4.31	3.37	10.0	2.46	4.16	—	—
ϕ Cen	121743	68245	3.80	B2 V	4.31	3.61	107.5	5.10	5.16	0.88	0.98
σ Cen	108483	60823	3.91	B2 V	4.31	3.36	169.0	2.97	3.27	1.34	1.27
V761 Cen	125823	70300	4.42	B2 V	4.31	3.25	5.0	—	—	—	—
13 Sco	145482	79404	4.57	B2 V	4.31	3.23	198.5	—	—	1.89	—
η Lup	143118	78384	3.41	B2.5 IV	4.27	3.51	241.0	6.57	6.06	—	—
HR 5471	129116	71865	4.00	B2.5 V	4.27	3.05	198.5	5.43	9.96	1.23	—
τ Lib	139365	76600	3.64	B2.5 V	4.27	3.26	100.0	4.63	4.82	—	—
θ Lup	144294	78918	4.20	B2.5 Vn	4.27	3.11	330.5	3.75	3.69	2.17	—
HR 4848	110956	62327	4.62	B2/3 V	4.27	2.91	11.0	—	—	1.24	1.94
ζ Cru	106983	60009	4.05	B2/3 V	4.27	2.95	151.5	2.61	2.67	0.47	2.22
η Cen	127972	71352	2.31	B2Ve	4.31	3.89	305.0	—	—	—	—
HR 5035	116087	65271	4.51	B3 V	4.23	2.80	223.0	—	—	1.57	2.14
ξ^2 Cen	113791	64004	4.27	B3 V	4.23	3.13	32.0	15.60	—	1.23	—
KT Lup	138769	76371	4.71	B3 V	4.23	2.88	106.0	—	—	—	—
ρ Cen	105937	59449	3.96	B3 V	4.23	2.80	147.0	—	—	0.61	1.12
HR 6214	150742	81972	5.63	B3 V	4.23	2.74	167.0	—	—	—	—
HR 5595	132955	73624	5.44	B3 V	4.23	2.72	10.0	—	—	—	—
HR 4732	108257	60710	4.81	B3 V(n)	4.23	2.88	298.0	4.81	4.75	—	—
λ Cru	112078	63007	4.60	B3 Vne	4.23	2.83	341.0	3.23	3.57	—	—
ρ Lup	128345	71536	4.05	B3/4 V	4.23	2.87	240.0	—	—	2.25	2.13
V863 Cen	105382	59173	4.47	B3/5 III	4.22	2.73	70.0	—	—	—	—
3 Cen	120709	67669	4.52	B4 III	4.22	2.75	0.0	3.70	—	—	—
HR 4549	103079	57851	4.99	B4 V	4.22	2.60	49.0	—	—	—	—
HR 4940	113703	63945	4.69	B4 V	4.22	2.79	216.0	3.17	3.11	1.76	1.59
V964 Cen	115823	65112	5.44	B5 III/IV	4.20	2.44	41.0	—	—	1.29	1.36
o Lup	130807	72683	4.31	B5 IV	4.20	2.91	51.0	—	—	1.10	0.34
π Lup	133242	73807	4.58	B5 V	4.20	2.94	202.5	—	—	1.54	1.47
ψ^2 Lup	140008	76945	4.72	B5 V	4.20	2.65	46.0	—	—	1.17	1.07
HR 5736	137432	75647	5.45	B5 V	4.20	2.56	130.0	—	—	2.13	1.15
π Cen	98718	55425	3.90	B5 Vn	4.20	2.96	351.5	5.21	2.94	2.27	2.33
μ^2 Cru	112091	63005	5.20	B5 Vne	4.20	2.46	124.0	2.97	—	0.62	1.07
V795 Cen	124367	69618	5.07	B5 Vne	4.20	2.62	301.0	2.77	2.72	1.87	—
HR 5967	143699	78655	4.89	B5/7 III/IV	4.16	2.58	175.0	5.93	—	1.12	1.06
HR 5625	133937	74100	5.82	B5/7 V	4.16	2.37	350.0	5.92	5.86	—	—
HR 6209	150591	81914	6.12	B6/7 V	4.15	2.39	271.0	4.54	6.47	1.89	1.94
HR 5753	138221	76048	6.49	B6/7 V	4.15	2.15	240.0	2.92	2.99	—	—

Table 1: Sample of B stars in Sco–Cen that have been observed by *TESS* (ordered by spectral type).

Name	HD	HIP	V	Sp. type	$\log(T_{\rm eff}/{\rm K})$	$\log(L/{\rm L}_\odot)$	$v \sin i$ (km s^{-1})	f_1 (d^{-1})	f_2 (d^{-1})	f_3 (d^{-1})	f_4 (d^{-1})
V1019 Cen	131120	72800	5.01	B7 II/III	4.15	2.68	60.0	—	—	—	—
V831 Cen	114529	64425	4.59	B7 V	4.15	2.62	216.0	—	—	—	—
GG Lup	135876	74950	5.60	B7 V	4.15	2.40	129.0	—	—	—	—
HR 5439	127971	71353	5.87	B7 V	4.15	2.03	191.0	5.42	3.04	2.25	2.18
—	147001	80142	6.50	B7 V	4.15	2.23	—	—	—	—	—
HR 5910	142250	77900	6.10	B7 V	4.15	2.24	15.0	2.54	2.50	—	—
HR 4706	107696	60379	5.37	B7 Vn	4.15	2.20	321.0	3.32	—	—	—
HR 4834	110506	62058	5.98	B7/8 V	4.12	2.08	178.0	2.71	2.76	1.28	0.43
HR 4879	111774	62786	5.97	B7/8 V	4.12	2.20	64.0	—	—	1.92	1.82
52 Hya	126769	70753	4.97	B7/8 V	4.12	2.44	199.5	2.98	2.92	0.45	0.51
HR 4290	95324	53701	6.18	B8 IV	4.10	1.91	55.0	5.52	—	—	—
HR 4089	90264	50847	4.99	B8 V	4.10	2.40	11.0	—	—	—	—
HR 4355	97583	54767	5.22	B8 V	4.10	2.07	178.0	—	—	1.90	1.85
FH Mus	110020	61796	6.25	B8 V	4.10	1.83	234.0	2.88	2.93	—	—
HR 5121	118354	66454	5.89	B8 V	4.10	2.16	253.0	—	—	1.33	1.38
—	126135	70455	6.96	B8 V	4.10	1.95	—	—	—	—	—
—	142256	77968	6.96	B8 V	4.10	1.95	—	3.75	3.81	—	—
HR 5207	120642	67703	5.26	B8 V	4.10	2.07	—	3.51	3.73	—	—
HR 6100	147628	80390	5.41	B8 V	4.10	2.25	160.0	2.54	2.59	—	—
HR 5579	132238	73341	6.47	B8 V	4.10	2.04	234.0	3.13	6.75	—	—
HR 5860	140784	77286	5.60	B8 V	4.10	2.16	364.0	3.05	2.95	—	—
HR 5449	128207	71453	5.74	B8 V	4.10	2.23	—	6.34	6.40	0.50	0.57
HR 6211	150638	81891	6.45	B8 V	4.10	2.02	166.0	—	—	—	—
μ Lup	135734	74911	4.27	B8 Ve	4.10	2.53	308.0	33.16	33.21	—	—
HR 4221	93563	52742	5.23	B8/9 III	4.06	2.47	249.0	—	—	1.15	1.10
HR 4913	112409	63210	5.16	B8/9 V	4.06	2.28	123.0	—	—	—	—
—	104080	58452	6.34	B8/9 V	4.06	1.85	—	—	—	—	—
—	128819	71724	6.65	B8/9 V	4.06	1.92	—	—	—	—	—
HR 4951	113902	64053	5.70	B8/9 V	4.06	1.87	249.0	—	—	—	—
HR 4748	108541	60855	5.44	B8/9 V	4.06	2.23	191.0	—	—	0.96	0.32
—	136482	75210	6.64	B8/9 V	4.06	1.83	—	3.57	3.62	—	—
—	143927	78754	7.06	B8/9 V	4.06	1.79	—	—	—	—	—
HR 5790	138923	76395	6.25	B8/9 V	4.06	1.90	271.0	3.32	3.37	—	—
—	151109	82154	7.00	B9 IV/V	4.03	1.76	—	3.65	3.61	—	—
HR 4692	107301	60183	6.19	B9 V	4.03	1.57	209.0	—	—	—	—
HR 4597	104600	58720	5.88	B9 V	4.03	1.76	214.0	3.33	3.38	—	—
HR 4832	110461	62026	6.06	B9 V	4.03	1.75	246.0	3.53	3.58	—	—
—	115583	65021	7.25	B9 V	4.03	1.65	—	3.38	3.24	—	—
HR 5230	121190	67973	5.71	B9 V	4.03	1.94	166.0	2.62	2.68	—	—
—	115988	65178	6.66	B9 V	4.03	1.65	—	2.85	—	—	—
HR 5294	123445	69113	6.17	B9 V	4.03	2.05	66.0	3.71	3.77	0.63	0.68
HR 5773	138564	76234	6.35	B9 V	4.03	1.55	154.0	—	—	—	—
12 Sco	145483	79399	5.67	B9 V	4.03	1.74	204.0	—	—	1.66	1.60
HR 5805	139233	76591	6.58	B9 V	4.03	1.77	209.0	—	—	—	—
HR 5400	126475	70626	6.35	B9 V	4.03	1.85	234.0	3.32	3.37	—	—
—	132094	73266	7.25	B9 V	4.03	1.67	—	—	—	—	—
—	141327	77523	7.46	B9 V	4.03	1.76	—	—	—	—	—
—	144591	79044	6.74	B9 V	4.03	1.65	—	—	—	—	—
—	149274	81208	6.64	B9 V	4.03	1.76	—	—	—	—	—
—	151726	82430	7.24	B9 V	4.03	1.64	—	—	—	—	—
HR 4874	111597	62683	4.89	B9 V	4.03	2.25	—	—	—	—	—
HR 5869	141168	77562	5.78	B9 V(n)	4.03	1.74	308.0	3.99	3.94	—	—
HR 5141	118991	66821	5.01	B9 Vn	4.03	1.91	321.0	3.20	2.63	—	—
—	104900	58901	6.20	B9 Vn	4.03	1.67	—	3.79	3.67	—	—
HR 4985	114772	64515	5.90	B9.5 V	4.02	1.79	249.0	2.61	3.64	—	—
—	104839	58859	6.47	B9.5 V	4.02	1.63	—	—	—	—	—

Table 1: Sample of B stars in Sco–Cen that have been observed by *TESS* (ordered by spectral type).

Name	HD	HIP	V	Sp. type	$\log(T_{\rm eff}/{\rm K})$	$\log(L/{\rm L}_\odot)$	$v \sin i$ (km s^{-1})	f_1 (d^{-1})	f_2 (d^{-1})	f_3 (d^{-1})	f_4 (d^{-1})
—	109195	61257	6.55	B9.5 V	4.02	1.62	—	—	—	—	—
—	115470	64892	6.79	B9.5 V	4.02	1.53	—	—	—	—	—
—	117484	65965	7.53	B9.5 V	4.02	1.42	—	—	—	—	—
—	123247	69011	6.42	B9.5 V	4.02	1.47	—	—	—	—	—
—	135454	74752	6.75	B9.5 V	4.02	1.60	—	—	—	—	—
—	137919	75915	6.33	B9.5 V	4.02	1.72	—	2.82	2.88	—	—
—	143022	78324	8.18	B9.5 V	4.02	1.22	—	—	—	2.18	2.24

This paper has been typeset from a TEX/LATEX file prepared by the author.